Grating-induced mode-splitting in an Al_2O_3 ring resonator

M. de Goede,[1] M. Dijkstra,[1] N. Acharyya,[2] G. Kozyreff,[2] and S.M. García-Blanco[1]

[1] Optical Sciences Group, MESA+ Institute for Nanotechnology, University of Twente, P.O. Box 217, 7500 AE Enschede, The Netherlands

[2] Optique Nonlinéaire Théorique, Université libre de Bruxelles (U.L.B.), CP 231, Belgium

Mode-splitting in a ring resonator can be achieved by mutual coupling of the two counter-propagating travelling resonance modes. This was realized by fabricating a Bragg grating in the cladding of a ring resonator. Mode-splitting of the resonance mode was observed, which could be harnessed for self-referenced sensing applications.

Whispering gallery modes inside a ring resonators have twofold degeneracy corresponding with two counter-propagating travelling waves at the same resonance wavelength. Mutual coupling between these two modes lifts their degeneracy and induces mode splitting of the resonance, resulting in two distinct resonances at different wavelengths (Fig. 1) [1,2,3]. Such mutual coupling can be achieved by inserting a reflective element inside the ring resonator that couples the clockwise mode into the counterclockwise mode and vice versa. A grating can be used to provide the coupling between the two counter-propagating travelling waves [4–6]. Then, the amount of wavelength splitting is directly linked to the reflective strength of the grating inside the ring resonator.

Here, a grating is implemented in an Al_2O_3 ring resonator to provide the reflective coupling necessary for achieving mode-splitting. This material was chosen for its low optical losses [7], simple integration on chip [8] and the possibility of rare-earth ion doping to achieve lasing and active functionalities [9]. Mode-splitting on an active device is of interest for the generation of radio frequencies that can be used for self-referenced, high-sensitivity analyte detection [10].

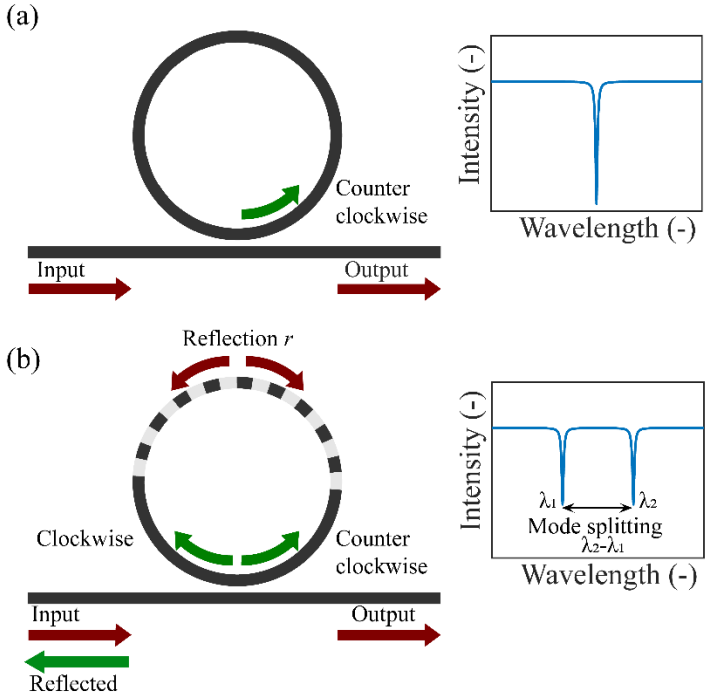

Fig. 1. Mode-splitting in a ring resonator. (a) Pristine ring resonator without grating has a degenerate resonance. (b) Grating-induced mutual coupling within a ring resonator induces mode-splitting, lifting the degeneracy of the resonance.

The protocol for the realization of a Bragg grating on an Al_2O_3 ring resonator was developed and based on forming the grating in a PMMA resist cladding layer. The grating is formed by covering the ring resonator in PMMA, followed by locally exposing it with electron beam. After development, periodic segments of PMMA are removed, leaving behind the Bragg grating on the ring resonator. An advantage of this method is that the PMMA grating is non-destructive and can easily be removed, allowing for a repeatable process.

The process is illustrated in Fig. 2(a) and starts with coating the ring resonator with PMMA (NANO^{TM} 950PMMA A4) by spinning it at 3.5k rpm for 1 minute to cover the device in a PMMA layer with a thickness of ~30 nm. This is followed by sputtering a Cr coating of 5 nm thick, to prevent charging during the electron beam exposure, since both the substrate and the sample are non-conductive. Then, the grating pattern is exposed on top of the ring resonator with a RAITH150 Two electron beam lithography tool, using a dose of 180 µC/cm^2 at an acceleration voltage of 10 kV. The grating design parameters were a period of 535 nm, patterning of the ring along 4/5 of its circumference, and a period filling fraction of 0.35 on the pattern mask. After patterning the Cr layer is removed by a wet etch of 10 seconds with a mixture of perchloric acid and ceric ammonium nitrate (TechniEtch Cr01), followed by rinsing it with deionized water. Then, the exposed PMMA is developed with a mixture of MIBK:IPA at a ratio of 1:3 for 40 seconds, after which the device is rinsed with IPA for 20 seconds and blown dry with N_2. The resulting grating was then imaged with SEM and AFM (Figs. 2 (b) and (c)). The resulting PMMA grating has a fill factor of ~0.5. A height profile of the PMMA grating shows that the teeth are ~30 nm thick (Fig. 2(d)), with some roughness being present.

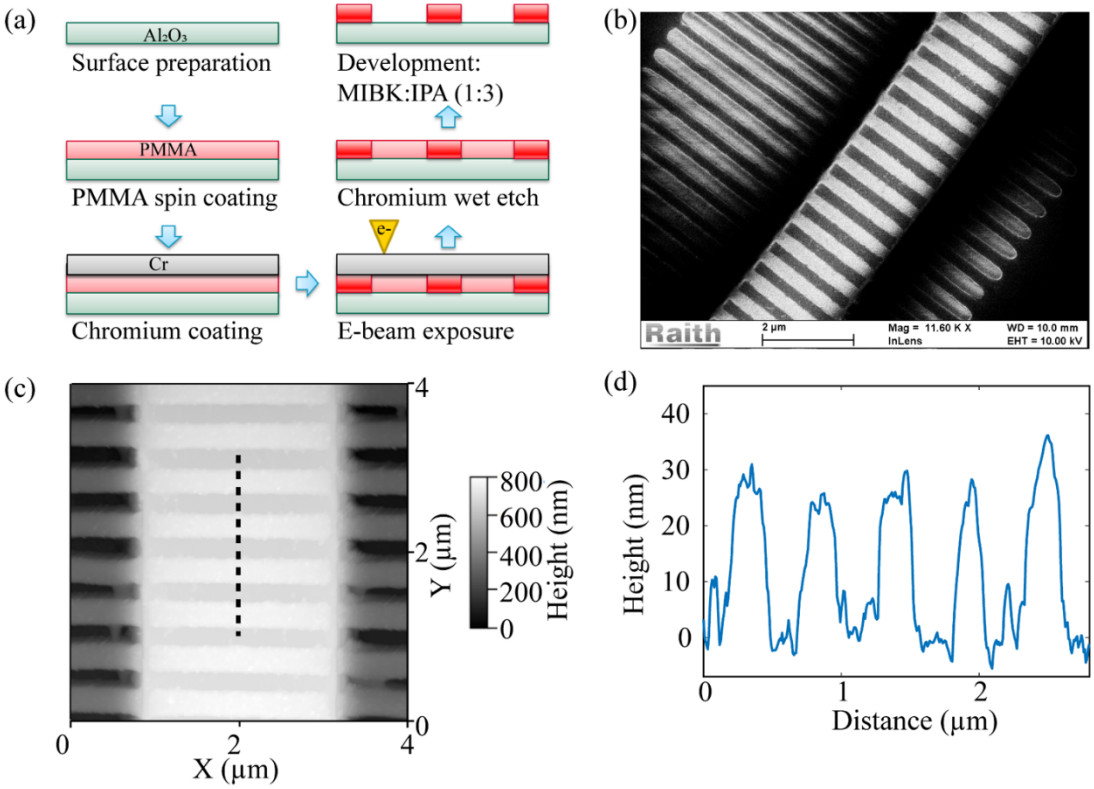

Fig. 2. Fabrication of the grating-integrated ring resonator. (a) Process flow of the fabrication of realizing a PMMA grating on top of the ring resonator waveguide. (b) SEM image of the developed PMMA grating. (c) AFM scan of the PMMA grating on top of a Al_2O_3 waveguide. (d) Height profile of the PMMA grating along the dotted line in (c).

To optically characterize the mode-splitting of the ring resonator with integrated Bragg grating, its transmission spectrum was recorded using an Agilent 81646 tunable laser. The sample was placed on a holder by vacuum contact and TE-polarized laser light was guided through a single

mode polarization maintaining fiber (PM1500-XP) and butt coupled to the sample using index-matching fluid. Figure 3 shows the transmission spectrum of the same device covered in PMMA before and after grating fabrication. Before grating fabrication, the spectrum of the ring resonator contains multiple degenerate sharp resonances in the wavelength range of 1600—1630 nm (Figs. 3 (a) and (b)). However, coupling of CW and CCW propagating modes via the grating fabricated on the ring resonator lifts the degeneracy and forms doublets of all the resonance modes in the bandwidth of the grating (Figs. 3 (c) and (d)). Since the reflectivity is a function of wavelength, the different resonances contain various amounts of mode-splitting throughout the wavelength range. For further analysis, the spectrum was normalized through a background subtraction and the resonance modes were fitted with either single or double Lorentzian functions, depending on whether the resonance mode was degenerate or not. The maximum mode-splitting lies around a wavelength of 1627 nm and amounts to ~410 pm or 46.5 GHz.

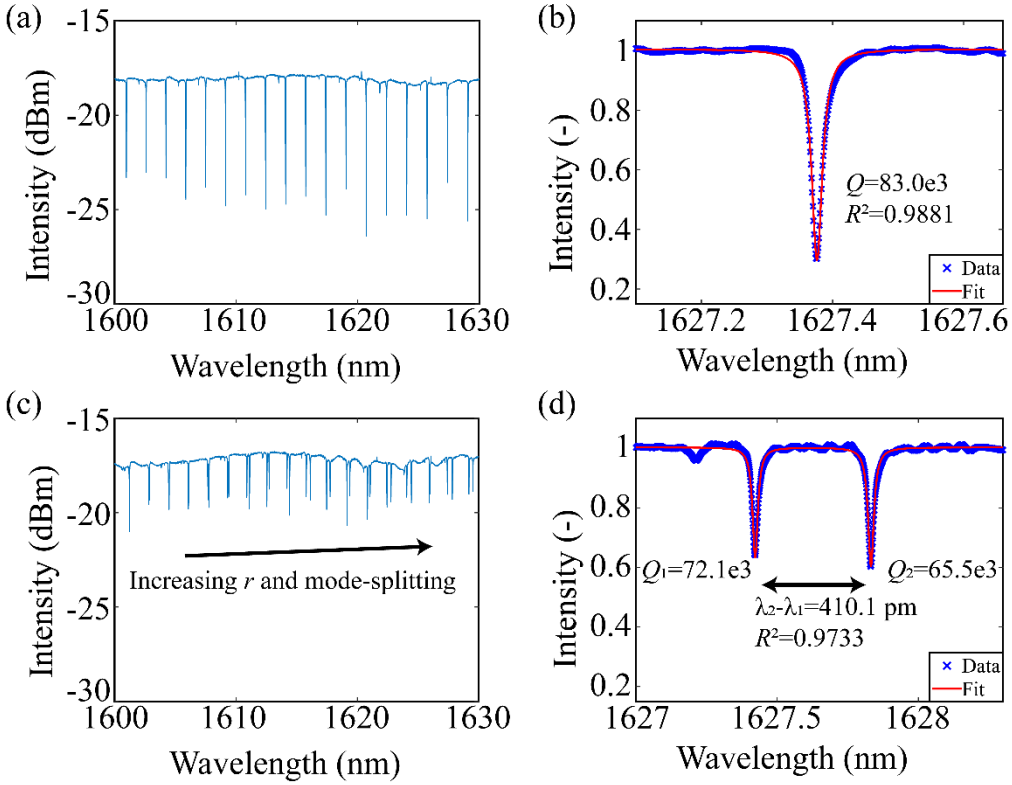

Fig. 3. Grating induced mode-splitting of a ring resonator. (a) Transmission spectrum of a ring resonator covered in PMMA before grating patterning and development. (b) Zoom and fit of degenerate resonance mode in (a). (c) Transmission spectrum of ring resonator after grating patterning and development. (d) Zoom and fit of non-degenerate resonance modes in (c), indicating the mode-splitting.

In conclusion, a Bragg grating was realized onto an Al_2O_3 ring resonator to achieve mode-splitting. The grating was fabricated by covering the ring resonator in PMMA and by locally removing grating teeth using electron beam lithography. A mode splitting of 410 pm was achieved, which was absent for a PMMA-covered ring resonator without the grating patterning and development. The mode-splitting could be used for self-referenced biosensing applications or the generation of radio frequencies in an active device.

References

1. D. S. Weiss, V. Sandoghdar, J. Hare, V. Lefèvre-Seguin, J.-M. Raimond, and S. Haroche, "Splitting of high-Q Mie modes induced by light backscattering in silica microspheres," Opt. Lett. **20**(18), 1835 (1995).
2. A. Mazzei, S. Götzinger, D. S. Menezes, G. Zumofen, O. Benson, and V. Sandoghdar, "Controlled coupling of counterpropagating Whispering-Gallery modes by a single

rayleigh scatterer: A classical problem in a quantum optical light," Phys. Rev. Lett. **99**(17), 1–4 (2007).
3. B. E. Little, J. P. Laine, and S. T. Chu, "Surface-roughness-induced contradirectional coupling in ring and disk resonators.," Opt. Lett. **22**(1), 4–6 (1997).
4. T. Wang, Z. Zhang, F. Liu, Y. Tong, J. Wang, Y. Tian, M. Qiu, and Y. Su, "Modeling of quasi-grating sidewall corrugation in SOI microring add-drop filters," Opt. Commun. **282**(17), 3464–3467 (2009).
5. Q. Huang, K. Ma, and S. He, "Experimental Demonstration of Single Mode- Splitting in Microring With Bragg Gratings," IEEE Photonics Technol. Lett. **27**(13), 1402–1405 (2015).
6. Z. Zhang, M. Dainese, L. Wosinski, and M. Qiu, "Resonance-splitting and enhanced notch depth in SOI ring resonators with mutual mode coupling," Opt. Express **16**(7), 4621 (2008).
7. J. D. B. Bradley, F. Ay, K. Wörhoff, and M. Pollnau, "Fabrication of low-loss channel waveguides in Al_2O_3 and Y_2O_3 layers by inductively coupled plasma reactive ion etching," Appl. Phys. B **89**(2–3), 311–318 (2007).
8. K. Worhoff, J. D. B. Bradley, F. Ay, D. Geskus, T. P. Blauwendraat, and M. Pollnau, "Reliable Low-Cost Fabrication of Low-Loss Al_2O_3:Er^{3+} Waveguides With 5.4-dB Optical Gain," IEEE J. Quantum Electron. **45**(5–6), 454–461 (2009).
9. E. H. Bernhardi, H. A. G. M. Van Wolferen, K. Wörhoff, R. M. De Ridder, and M. Pollnau, "Highly efficient, low-threshold monolithic distributed-Bragg-reflector channel waveguide laser in Al_2O_3:Yb_{3+}," Opt. Lett. **36**(5), 603–605 (2011).
10. B.-B. Li, W. R. Clements, X.-C. Yu, K. Shi, Q. Gong, and Y.-F. Xiao, "Single nanoparticle detection using split-mode microcavity Raman lasers," Proc. Natl. Acad. Sci. **111**(41), 14657–14662 (2014).